Electrical Conductivity of Ceria-Based Oxide/Alkali Carbonate Eutectics Nanocomposites

Mizuhata, Minoru
Kubo, Hiroshi
Ichikawa, Yudai
Maki, Hideshi
Matsui, Masaki

(Invited) Electrical Conductivity of Ceria-Based Oxide/Alkali Carbonate Eutectics Nanocomposites

ECS Transactions, 98 (10) 63-71 (2020)
10.1149/09810.0063ecst ©The Electrochemical Society

Electrical Conductivity of Ceria-based Oxides/ Alkali Carbonate Eutectics Nanocomposites

Minoru Mizuhata[a,b], Hiroshi Kubo[a], Yudai Ichikawa[a],
Hideshi Maki[a,c], and Matsui Masaki[a]

[a] Department of Chemical Science and Engineering, Graduate School of Engineering, Kobe University, Kobe 657-8501, Japan
[b] Faculty of Chemistry, Jagiellonian University ul. Gronostajowa 2, 30-387 Kraków, Poland
[c] Environment Management Center, Kobe University, Kobe 657-8501, Japan

Thermal properties and the electrical conductivity for the SDC / ternary carbonate coexisting system was measured and the influence of the solid phase was discussed. In the ceria-based oxide/carbonate coexistence system, the melting enthalpy of carbonate disappeared when the liquid phase volume fraction was less than 45 vol%, and the melting point decreased due to the influence of the solid phase. The activation energy of conductivity increases in the region where the apparent average thickness is approximately 0.5 nm or less, the carbonate is significantly affected by the solid phase in a very narrow range, and the ceria-based oxide causes ion migration in the interface layer. It became clear that it did not inhibit. From these results, it was clarified that the low temperature characteristics are remarkably improved although the influence of the solid phase on the ionic conduction is limited.

Introduction

At present, the problems of global warming and depletion of fossil fuels have become major problems on a global scale. There is a need for a highly efficient power generation device that does not emit greenhouse gases such as carbon dioxide. In particular, there is an advantage that high-temperature fuel cells such as solid oxide fuel cells (SOFC) and molten carbonate fuel cells (MCFC) operate at high temperatures, so they are highly efficient and do not require expensive precious metal catalysts such as platinum as electrode materials (1). However, operation at high temperature leads to deterioration of the cell and is not suitable for long-term use. Therefore, in order to reduce the corrosion and improve the durability of the materials in the cell equipment, numerous research for the eutectic molten salt composite with fine powder at lower temperature operations have been carried out. Yttria-stabilized zirconia (YSZ) has been used as the electrolyte material for conventional SOFCs, but the operating temperature must be 1273 K or higher to obtain sufficient electrical conductivity when YSZ is used as the electrolyte. So, trivalent Sm and Gd-doped ceria-based oxides (SDC or GDC) are of interest. It is known that ceria has oxygen ion conductivity by doping with trivalent ions like zirconia, and has sufficient oxygen ion conductivity even in the intermediate temperature range of 773-973 K. However, Ce^{4+} is easily reduced to Ce^{3+} under H_2 atmosphere and shows electron conductance (2). Furthermore, it is known that the open circuit voltage is reduced and the

electrolyte is reduced and expanded due to electron conduction, and it is difficult to use it as a single electrolyte at a sufficiently high temperature.

In recent years, a ceria-based oxide/carbonate composite electrolyte obtained by adding a carbonate having an electron-insulating property to a ceria-based oxide has attracted attention. In such a composite electrolyte, the molten carbonate is used in a state of being impregnated with the oxide, and an interface layer is formed between the solid oxide and the carbonate due to the interaction between the solid and the liquid. This interface layer is considered to play an important role in improving the electrical conductivity, and it is considered that a behavior of carbonate different from that of bulk (3-6). H^+, O^{2-}, and CO_3^{2-} are considered as the ionic species for ionic conduction in the ceria-based oxide/carbonate composite electrolyte, which shows high ionic conduction in the medium temperature range (673-1023 K). Among these ionic species, H^+ and O^{2-} are considered to have ion conduction paths in the interface layer, and the mechanism of ion conduction called the Swing model or "gear" mechanism was proposed(7-9). Although these ionic conduction mechanisms are rational to explain the improvement of ionic conduction, little detailed research has been done on the state of carbonate at the interface. Therefore, further studies are needed on the behavior of carbonates on solid surfaces and how the interactions contribute to ionic conduction at intermediate temperatures. Therefore, the behavior of carbonates existing in the vicinity of solids has been investigated using a ceria-based oxide having a large specific surface area synthesized by the Pechini method, which is one of the complex polymerization methods, in the solid phase (10, 11). We have been using Sm-doped CeO_2 (SDC), which is a ceria-based oxide doped with CeO_2 and Sm at a ratio up to 20 mol%, and a composite material using a eutectic salt of alkali-metal carbonates. As a result of thermophysical property measurement and electric conductivity measurement, it has been reported that the molten carbonate is affected by the solid phase, the enthalpy of fusion disappears, and contributes to the electric conductivity at lower temperature (12). In this study, CeO_2 and SDC nanoparticles prepared by the Pechini method (11) were used as the ceria-based oxide, and eutectic salts of Li_2CO_3, Na_2CO_3, and K_2CO_3 (LNK) were used as the carbonate. We measured thermal properties and the electrical conductivity for the SDC / ternary carbonate coexisting system and discussed the influence of the solid phase.

Experimental

Samples

Preparation of nanoparticles of CeO_2 and SDC. Cerium nitrate hexahydrate ($Ce(NO_3)_3 \cdot 6H_2O$ (Nacalai Tesque, Inc.) and samarium nitrate hexahydrate ($Sm(NO_3)_3 \cdot 6H_2O$ manufactured by Nacalai Tesque, Inc.) were dissolved in deionized distilled water, and a predetermined amount of citric acid (Nacalai Tesque, Inc.) aqueous solution and ethylene glycol (Nacalai Tesque, Inc.) was added as written in Ref.11 (11). An organic precursor was obtained by heating at 333 K for 12 hours and then at 573 K for 12 hours. Further, the precursor was calcined under air atmosphere at 673 K for 4 hours and vacuum dried at 473 K for 3 hours to obtain CeO_2 and SDC10 and SDC20 with Sm ratio of 10 and 20 mol %. The obtained oxide sample was stored in a glove box under an argon atmosphere.

Preparation of LNK eutectic carbonate. Lithium carbonate (Li_2CO_3: Nacalai Tesque Co., Ltd.), sodium carbonate (Na_2CO_3 : Kishida Chemical Co., Ltd.) and potassium carbonate (K_2CO_3: Nacalai Tesque Co., Ltd.) were used. It was dried for 48 hours under

CO_2 atmosphere at 473 K, respectively and kept in a glove box under an argon atmosphere. These carbonates were mixed so that the eutectic composition was Li_2CO_3:Na_2CO_3:K_2CO_3=32:35:33 in weight ratio, corresponded to $(Li_{0.435}Na_{0.315}K_{0.25})_2CO_3$, and this carbonate is abbreviated as LNK hereinafter. Table 1 shows the physical properties of LNK. The eutectic point is 670 K and Density is 2.32 gcm^{-1} (13).

Preparation of samples for measurement of ac impedance. LNK was mixed with CeO_2 or SDC using an agate mortar under an argon atmosphere so as to have a predetermined liquid phase volume fraction, to obtain LNK-CeO_2 or LNK-SDCs. The liquid volume fraction; φ, was calculated by the following equation.

$$\varphi = \frac{w_{salt} / d_{salt}}{w_{salt} / d_{salt} + w_{solid}/d_{solid}} \quad [1]$$

where w_{salt}, d_{salt}, w_{solid} and d_{solid} in the above equation are the weight and density of the carbonate melt, the weight and density of the solid phase, respectively. The mixed sample was pressure-formed at 60 MPa for 30 minutes, heated at 773 K in a carbon dioxide atmosphere for 1 hour, and the solid phase was impregnated with carbonate to prepare a tablet-shaped sample (12).

Evaluation of solid phase samples

SEM shape observation. A field emission scanning electron microscopy (FE-SEM) was used for surface observation of the prepared CeO_2 and SDC using JSM-6335F (JEOL Ltd). The accelerating voltage of the electron beam at the time of measurement was set to 15 kV, and in order to prevent the sample surface from being charged up, a carbon coater (Meiwa Shoji CC-40FM) was applied to the sample surface before observation.

Specific surface area. To measure the specific surface area of the prepared sample, a high-speed specific surface area/pore distribution measuring device (NOVA-2200e Quantachrome, Inc., USA) was used, and nitrogen adsorption/desorption isotherm was measured at 77 K in a relative pressure range of 0.05-0.1. As a pretreatment of the sample, it was dried in vacuum at 473 K for 5 hours. The specific surface area was determined by the BET method as an analytical method.

XRD measurement. X-ray diffraction measurement was performed on the prepared CeO_2 and SDC by the following method. For the measurement, X-ray diffraction measurement was performed using a fully automatic multipurpose horizontal X-ray diffractometer (Rigaku Smart Lab). The apparatus was set up with a tube voltage of 45 kV, a tube current of 200 mA, and the X-ray source was a CuKα1 (λ = 1.541Å) wire for the concentrated method. The measurement conditions were θ = 10 - 100°, scan speed; 2.0°/min, and scan step; 0.01°.

Evaluation of carbonate/ceria-based oxide coexisting system

Differential Thermogravimetric Analysis (TG-DTA). Using Thermo Plus Evo TG 8120 manufactured by Rigaku Corporation, thermal analysis was performed using α-Al_2O_3 as a Ref 12 [12]. The measurement conditions were temperature range 373-773 K, heating

rate 5 K/min, CO_2 atmosphere, and DTA range 100 μV.

AC impedance measurement. The electrical conductivity of the sample was measured by the AC impedance method. Figure 1 shows a schematic diagram of the electrochemical measurement device. A Hewlett Packard 4284A precision LCR meter was used for the measurement of the prepared tablet-shaped sample, and the electrode was an Au-Pd electrode (diameter: 10 mm, Au:Pd =90:10) was used. The measurement conditions were CO_2 flow (0.1 MPa, 50 ml/min), frequency range 25 Hz-1 MHz, temperature range 573-773 K, and applied voltage 0.6 V. In addition, the ionic conductivity was measured during heating process, and the data was analyzed using impedance analysis software (ZView Version 3.1c).

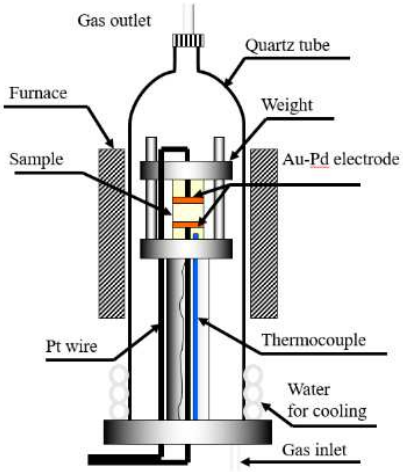

Figure 1. Apparatus for electric conductivity measurement.

Results and Discussion

Evaluation of fabricated CeO_2 and SDC

SEM observation. Figure 2 shows SEM images of CeO_2, SDC10, and SDC20. From these SEM images, it was confirmed that the particle size of both CeO_2 and SDC was about several tens nm, and the shape and particle size were not affected by the solid solution of Sm^{3+}.

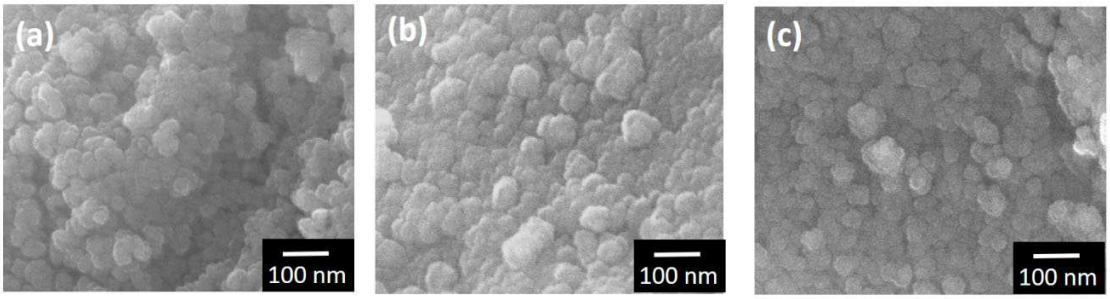

Figure 2. SEM images of CeO_2 and SDCs nanoparticles (a) CeO_2 (b) SDC10 (c) SDC20.

Evaluation of specific surface area by BET method. Table I shows the specific surface area obtained by the BET method. Similar to the shape, no proportional relationship was found between the solid solution of Sm^{3+} and the specific surface area, and it was confirmed that both CeO_2 and SDC have the same large specific surface area.

Table I. Specific surface area and density of powder sample.

Samples	Specific surface area/m^2g^{-1}	Density/gcm^3
CeO_2	90.1	7.09
SDC10	70.2	7.14
SDC20	63.1	6.96

XRD measurement. XRD measurement was performed to examine the crystal structures of the prepared CeO_2 and SDC. Fig. 3 (a) shows the XRD measurement results of each sample. The diffraction pattern assigned to CeO_2 indexed in ICDD PDF-4 database #34-0394 was confirmed for all the samples. Fig. 3(b) shows the magnified diffraction patterns assigned to the 111 plane of CeO_2, SDC10, and SDC20. In each diffraction pattern, it was confirmed that as the doping amount of Sm3+ increased, it shifted to the lower angle side. It is considered that this is because the ionic radius of Sm^{3+} was larger than that of Ce^{4+}, so that the interplanar spacing was widened, and it was confirmed that Sm^{3+} was properly doped.

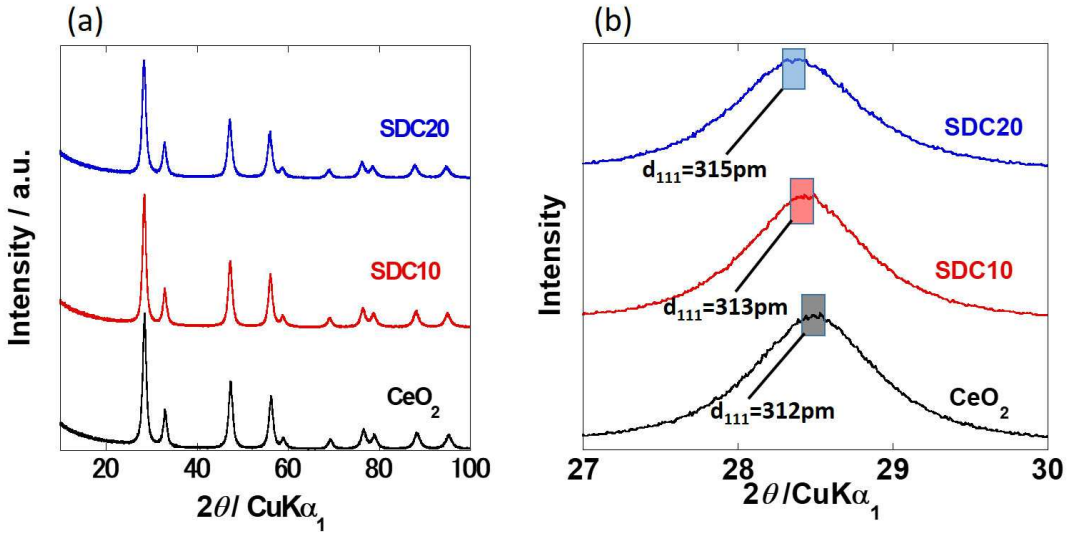

Figure 3. (a)XRD patterns and (b) detail profile for 111 of CeO_2 and SDCs nanoparticles.

Evaluation of LNK-CeO_2 and LNK-SDCs

Thermal analysis. In order to observe the phase transition of carbonate near the solid, thermal analysis measurement was performed in the ceria-based oxide/carbonate coexisting system. Figure 4 shows the DTA curve in the coexisting system of LNK and CeO_2, SDC10 and SDC20. In any system, the enthalpy change due to the melting of carbonate was not confirmed at the liquid phase volume fraction of 15-45 vol%, but appeared slightly at 55 vol%. Comparing with the past results of composite materials using eutectic salt of Li_2CO_3 and Na_2CO_3 in the liquid phase, enthalpy change due to melting

was confirmed even at liquid phase volume fraction of 35 vol% [12], and carbonate It is considered that the change from binary system to ternary system caused a change in the interaction between the solid phase and the liquid phase, resulting in a change in the liquid phase volume fraction where an endothermic peak appeared.

It is considered that the interaction between the solid phase and the liquid phase changed due to the change of the carbonate from the binary system to the ternary system, and the liquid phase volume fraction where the endothermic peak appeared changed. The eutectic point of LNK was found to be 671 K, and it was confirmed that the eutectic point was shifted to the low temperature side by the influence of the solid phase when mixed with CeO_2, SDC10, and SDC20. Also, at 45 and 55 vol% of LNK-SDC20, the ternary carbonate phase-separates into $LiKCO_3$, $LiNaCO_3$, etc., and each melts independently, resulting in a peak around 660 K and a peak of 690 K. It is considered that a slight change in enthalpy could be confirmed. From these results, it is considered that the larger the amount of Sm^{3+} doped, the easier the phase separation of carbonate, and the greater the influence on the thermal properties of carbonate.

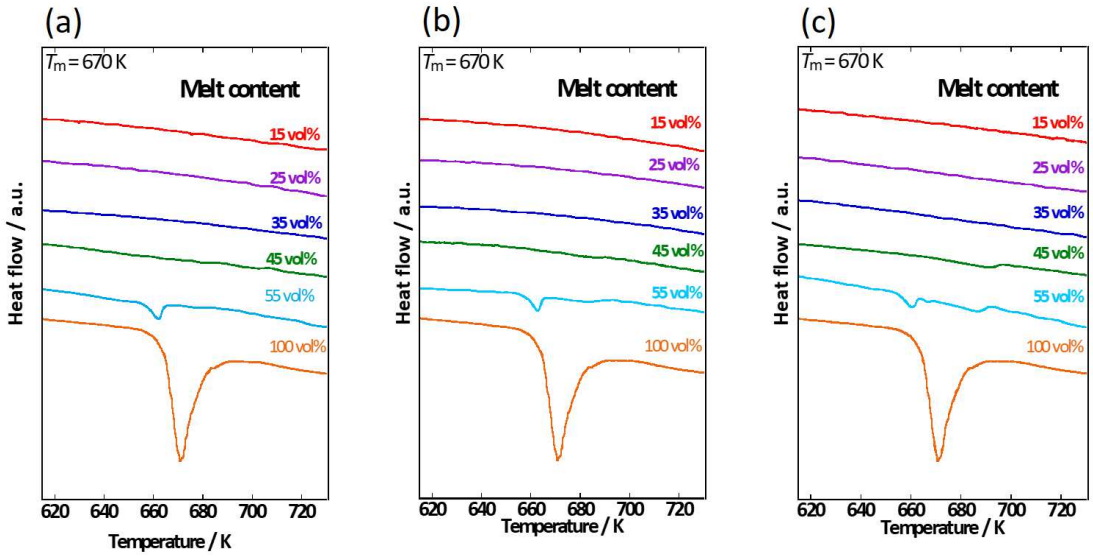

Figure 4. DTA curves of LNK coexisting with (a)CeO_2(90.1 m^2 g^{-1}), (b)SDC10 (70.2 m^2 g^{-1}), (c)SDC20 (63.1 m^2 g^{-1}) for each melt contents.

AC impedance measurement. Figure 5 shows the temperature dependence of ionic conductivity in the ceria-based oxide/carbonate coexisting system obtained from the results of AC impedance measurement. In LNK-CeO_2, only a few inflection points due to melting of the molten salt were observed in the samples with a liquid volume fraction of 35 vol% or less. At temperatures below the inflection point, the conductivity of 55 vol% is lower than the value of 25-45 vol%.This is because there is no inflection point in the 25 and 35 vol% sample, so it exists at the solid interface even below the eutectic point. This is because the carbonate that was used was in a molten state and the conductivity did not decrease even at low temperatures. In addition, inflection points associated with melting were observed in LNK-SDC10 at a liquid volume fraction of 15-55 vol% and in LNK-SDC20 at 45 and 55 vol%. In all systems, the inflection point associated with the melting of carbonate was confirmed at about 645 K, which was shifted to a temperature lower than

the melting point of the eutectic carbonate, similar to the measurement results of thermal analysis. It suggests that it was greatly influenced by the solid phase. In addition, in any of the samples with low liquid volume fraction, the temperature dependence of the electrical conductivity follows the VTF equation, and continuous bending is observed. This is considered to be bending due to the influence of free volume, such as the viscosity of the molten carbonate increasing due to the glass transition. Especially in the system of LNK-SDC20 composite, it was shown that the temperature dependence of VTF type with strong bending and the increase of T_0 were accompanied with the increase of the doping amount of Sm^{3+}.

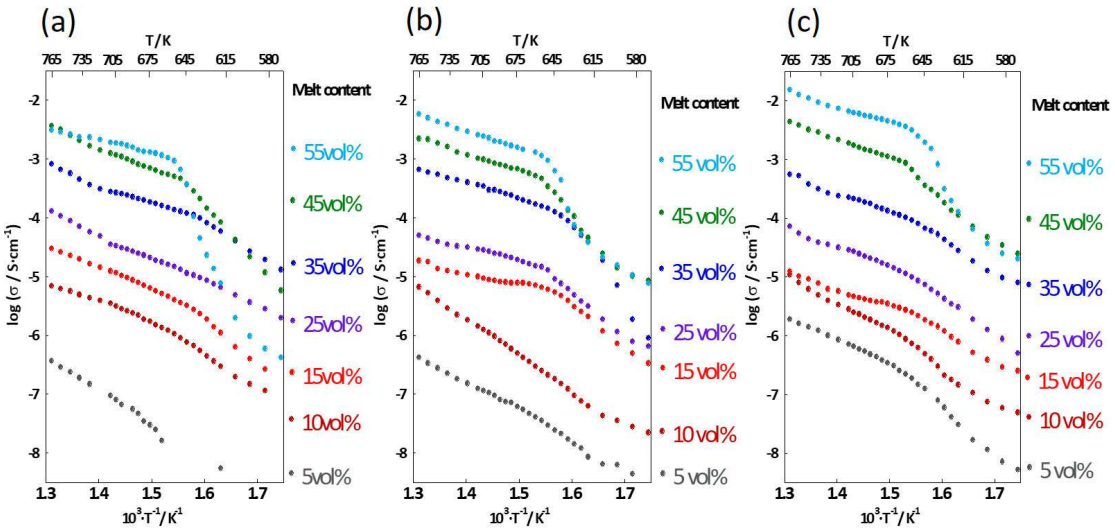

Figure 5. Temperature dependence of electrical conductivity for LNK coexisting with (a)CeO_2(90.1 m^2 g^{-1}), (b)SDC10 (70.2 m^2 g^{-1}), and (c)SDC20 (63.1 m^2 g^{-1}).

Apparent average thickness and activation energy. Introducing the apparent average thickness to estimate how far the effect of the solid phase will reach in the liquid phase. Apparent average thickness is defined as

[Apparent average thickness]
= [Total volume of liquid phase] / [Total surface area of solid phase] [2]

It has a dimension of length and represents the thickness of the liquid layer on the solid surface.The activation energy was calculated from the graph in Fig. 5 using the following VTF equation.

$$\log \sigma = AT^{-1/2} \exp[-B/(T-T_0)] \quad [3]$$

where T_0 is the glass transition point, and A and B are constants. Figure 6 shows a graph of the relationship between the apparent average thickness of the liquid phase and the activation energy of electrical conductivity; ΔE_a. The activation energy; ΔE_a, increased as the apparent average thickness decreased, and increased sharply in the region where the apparent mean thickness was about 0.5 nm or less. Therefore, it was revealed that carbonate was significantly affected by solids in a very narrow range, suggesting that the ceria-based oxide did not inhibit ion transfer in the interfacial layer.

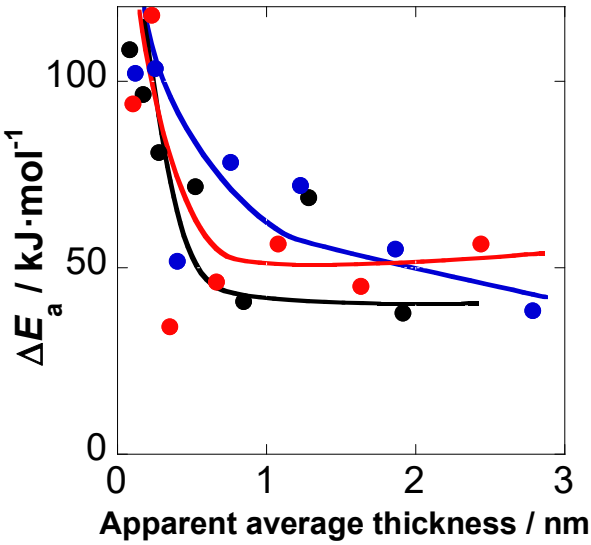

Figure 6. The variation of activation energy; ΔE_a, of the electrical conductivity with apparent average thickness for Ceria-based oxide / LNK composite systems.

Dependence of conductivity on liquid content. Fig. 7 shows changes in conductivity at various temperatures depending on the liquid volume fraction. At 673 K and 723 K, all carbonates were in a molten state, so that the conductivity increased as the amount of liquid phase increased in all these systems due to the increase in the number of carrier ions moving in the electrolyte. On the other hand, at the temperature below the eutectic point (623 K, 583 K), the maximum conductivity was confirmed. When the liquid phase volume fraction is high, a large amount of bulk carbonate is present, and in the region below the eutectic point, many parts are crystallized. Ionic conduction is difficult to occur in this region, and the ions melt even at low temperatures at the solid-liquid interface It is considered that the region moves in the state, and by increasing the solid phase, the region in the molten state is maintained toward lower temperate range, the conductivity increases, and the conductivity becomes maximum. In LNK-CeO_2, maximum values appeared at 623 K at 45 vol% and at 583 K at 35 vol%.

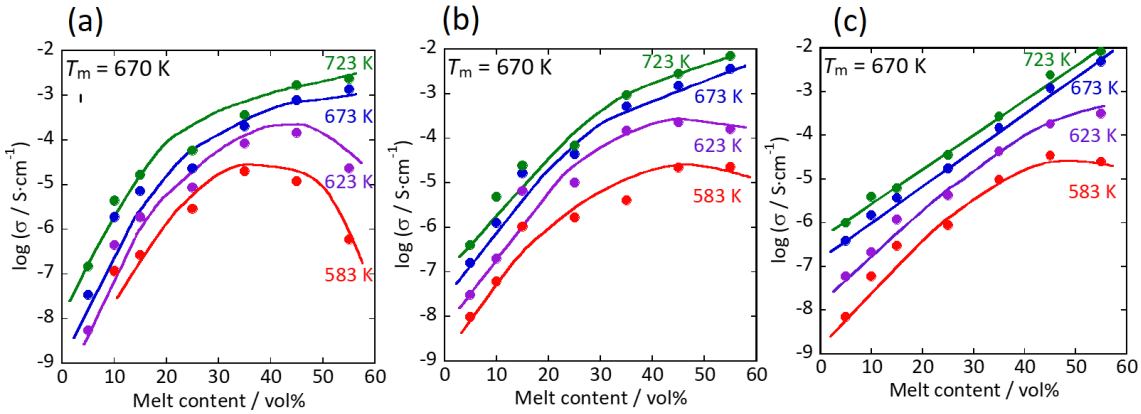

Figure 7. Variation of conductions for LNK coexisting with (a)CeO_2(90.1 m^2 g^{-1}), (b)SDC10 (70.2 m^2 g^{-1}), and (c)SDC20 (63.1 m^2 g^{-1}) at various temperatures.

It is considered that the conductivity was decreased because the number of carrier ions was decreased and the conduction path was interrupted when the solid phase was further increased. However, in LNK-SDC10 and LNK-SDC20, ions do not move easily even if the solid phase is increased due to the effect of the free volume of the molten carbonate due to the glass transition, the conductivity does not rise so much, and the maximum value like LNK-CeO[2]. It is believed that it did not appear clearly. In addition, since the position of the maximum value shifts to the larger liquid phase volume fraction as the Sm^{3+} content increases, it is suggested that the conductivity is affected by the Sm^{3+} content of the coexisting solid oxide.

Summary

Thermal properties and the electrical conductivity for the SDC / ternary carbonate coexisting system was measured and the influence of the solid phase was discussed. From the DTA measurement results, it was confirmed that in the ceria-based oxide/carbonate coexistence system, the melting enthalpy of carbonate disappeared when the liquid phase volume fraction was less than 45 vol%, and the melting point decreased due to the influence of the solid phase. From the results of AC impedance measurement, the inflection point due to melting was about 645 K in all systems, but there was a difference in the liquid phase volume fraction where the inflection point appeared, and there was a difference in the mutual interaction with carbonate due to Sm^{3+} doping. It was suggested that the action changed and that the higher the proportion of Sm^{3+}, the more the temperature dependence of VTF type was shown. In addition, the activation energy greatly increases in the region where the apparent average thickness is approximately 0.5 nm or less, the carbonate is significantly affected by the solid phase in a very narrow range, and the ceria-based oxide causes ion migration in the interface layer. It became clear that it did not inhibit From these results, it was clarified that the low temperature characteristics are remarkably improved although the influence of the solid phase on the ionic conduction is limited.

References

1. N. Laosiripojana and S. Assabumrungrat, *J. Power Sources*, **163**, 943 (2007).
2. D. J. L. Brett, A. Atkinson, N. P. Brandon, and S. J. Skinner, *Chem. Soc. Rev.*, **37**, 1568 (2008).
3. M. Mizuhata and S. Deki, *J. Rare Earths*, **23**, 1 (2005).
4. M. Mizuhata T. Ohta, and S. Deki, *Electrochemistry*, **77**, 721 (2009).
5. M. Mizuhata, T. Ohashi, and A. B. Bèlèkè, *Int. J. Hydrog. Energy*, **37**, 19407 (2012).
6. M. Mizuhata, K. Takeda, and H. Maki, *ECS Trans.*, **64(4)**, 45 (2014).
7. X. Wang, Y. Ma, S. Li, A.-H. Kashyout, B. Zhu, and M. Muhammed, *J. Power Sources*, **196**, 2754 (2011).
8. C. Qin and A. Gladney, *Comput. Theor. Chem.*, **999**, 179 (2012).
9. X. Lei, K. Haines, K. Huang, and C. Qin, *J. Power Sources*, **305**, 161 (2016)
10. L. Spiridigliozzi, M. Biesuz, G. Dell'Agli, E. Di Bartolomeo, F. Zurio, and V. M. Sglavo, *J. Mater Sci.*, **52**, 7479 (2017).
11. P. Ramos-Alvarez, M. E. Villafuerte-Castrejon, G. Gonzalez, M. Cassir, and C. Flores-Morales, J. A. Chavez-Carvayar, *J. Mater. Sci.*, **52**, 519 (2017).
12. M. Mizuhata, H. Kubo, H. Maki, and M. Matsui, *ECS Trans.*, **86(14)**, 101 (2018).
13. M. Kenisarin, *Renew. Sust. Energ. Rev.*,**14**, 955 (2010).